Periodico di Mineralogia (2011), 80, 1 (Special Issue), 145-153 DOI: 10.2451/2011PM0012

PERIODICO di MINERALOGIA
established in 1930

An International Journal of
MINERALOGY, CRYSTALLOGRAPHY, GEOCHEMISTRY, ORE DEPOSITS, PETROLOGY, VOLCANOLOGY
and applied topics on *Environment*, *Archeometry* and *Cultural Heritage*

Special Issue in memory of Sergio Lucchesi

In situ high-temperature X-ray powder diffraction study of the synthetic $Ca_2Sb_2O_7$ weberite-type compound

Laura Chelazzi[1], Tiziana Boffa Ballaran[2], Luca Bindi[3, 4] and Paola Bonazzi[1, 4,*]

[1]Dipartimento di Scienze della Terra - Università di Firenze, Italy
[2]Bayerisches Geoinstitut, Universität Bayreuth, Germany
[3]Museo di Storia Naturale, Sezione di Mineralogia, Università di Firenze, Italy
[4]C.N.R. - Istituto di Geoscienze e Georisorse - Sezione di Firenze, Italy
[*]Corresponding author: *paola.bonazzi@unifi.it*

Abstract

The crystal structure of synthetic $Ca_2Sb_2O_7$ has been investigated by in situ X-ray powder diffraction methods within the temperature range 298-1273 K. $Ca_2Sb_2O_7$ is orthorhombic, space group *Imma*, over the entire temperature range and shows only general thermal expansion. The unit-cell parameters show a monotonous increase as a function of temperature. Only slight changes occur in the individual bond distances without evidence of abrupt structural changes. The mean coefficients of thermal expansion along the various axes are: $\alpha_a = 9.49 \times 10^{-6}\ K^{-1}$, $\alpha_b = 10.11 \times 10^{-6}\ K^{-1}$, $\alpha_c = 7.56 \times 10^{-6}\ K^{-1}$ and the bulk thermal expansion coefficient $\alpha_V = 27.20 \times 10^{-6}\ K^{-1}$.

Key words: weberite; $Ca_2Sb_2O_7$; X-ray powder diffraction; Rietveld refinements.

Introduction

Most of the natural and synthetic $A_2B_2X_7$ compounds (A = medium-large cations; B = octahedrally coordinated, high-charge cations; X = O^{2-}, F^-) adopt a zirconolite-polytype (commonly pyrochlore-like) or a weberite-polytype structure, depending on the kind of cations (ionic radius, electronegativity, etc.), as well as on the pressure and/or temperature of crystallization. Both zirconolite-type and weberite-type $A_2B_2X_7$ compounds can be described as a sequence of A_3B- and AB_3-pyrochlore-type layers, named *M* and *N* respectively following the notation used by Mazzi and Munno (1983). In both cases, A and B cations form a distorted face-centered cubic array. The anion distribution over 7/8 of the tetrahedral cavities of the A_2B_2 array observed in pyrochlore and in the zirconolite-type compounds, is not maintained in weberite-type compounds, where one of the anions moves from a tetrahedral interstice to an adjacent octahedral interstice. This arrangement, as well illustrated by Grey et al. (2003), is a common feature of all weberite-type polytypes.

Polytypic relationships based on different stacking sequences of the *M* and *N* layers are common in both zirconolite-type (Gatehouse et al., 1981; Mazzi and Munno, 1983; Smith and Lumpkin, 1993; Coelho et al., 1997) and weberite-type (Giuseppetti and Tadini, 1978; Yakubovich et al., 1994; Grey and Roth, 2000; Bonazzi and Bindi, 2007) structures.

The driving forces controlling a given compound to crystallize in one of these two competing structural types (i.e., weberite- or zirconolite-type) are still scarcely known. As for weberite-type structures, Cai and Nino (2009) hypothesized that the stabilization of a polytypic variant may be related to the relative size of the A and B cations; among the $A_2^{2+}Sb_2O_7$ oxides, the mineral ingersonite (A^{2+} = 3/4Ca + 1/4Mn - Bonazzi and Bindi, 2007) and the synthetic $Mn_2Sb_2O_7$ (Scott, 1990) crystallize with the weberite-3*T* structure, while $Sr_2Sb_2O_7$ and $CaPbSb_2O_7$ crystallize with the weberite-2*O* structure (Cai and Nino, 2009 and references therein). According to Ismunandar and Budiman (2002), $Pb_{2.5}Sb_{1.5}O_{6.75}$ adopts a pyrochlore structure at room temperature and transforms to an orthorhombic structure above 1023 K. Under ambient-pressure conditions, $Ca_2Sb_2O_7$ crystallizes as a cubic pyrochlore below 973 K, above which it adopts an orthorhombic weberite structure (Brisse et al., 1972); moreover, the cubic structure is reported to form by synthesis at pressures higher than 6 GPa (Knop et al., 1980). As a part of an investigation of stability of weberite-type antimonates and their behaviour as a function of temperature, pressure and chemistry, it is here reported an in situ HT-XRPD study of the synthetic $Ca_2Sb_2O_7$ weberite-type compound.

Synthesis method and X-ray powder diffraction

Syntheses of $Ca_2Sb_2O_7$ were performed by using a standard solid-state reaction technique from appropriate mixture of $CaCO_3$ and Sb_2O_3 (Aldrich-99%). The ground mixtures were heated in air in platinum crucibles at 1373 K for 84 h. Run charges were allowed to cool slowly in the furnace down to room temperature.

The microcrystalline products thus obtained were characterized by X-ray powder diffraction. Data were collected with a Philips *X'Pert Pro* X-ray diffraction system equipped with a PANanalytical solid state detector, operating in reflection mode, with Co$K\alpha_1$ (λ = 1.78897 Å) radiation selected with a focusing monochromator and with a symmetrically cut curved Johansson Ge(111) crystal. X-ray data were collected over a range $20 < 2\theta < 110°$ from room temperature up to 1273 K, with silicon as temperature internal standard (Swenson, 1983), using a high-temperature chamber Anton Paar HTK 1200. Scan-step and counting time were 0.03° and 3 s/step, respectively.

Unit-cell parameters at room temperature were: a = 7.3043(2), b = 10.2253(4), c = 7.4611(2) Å, V = 557.26(2) Å^3. Subsequently, the temperature was raised to 323 K with a heating rate of 5 °/min and the powder pattern was collected again. The same procedure was then repeated at 373, 473, 573, 673, 773, 873, 1073, 1173, and 1273 K. Before each measurement the sample was held at the specified temperature for 30 min.

Rietveld refinements

Structural refinements were performed with the Rietveld analysis program GSAS (Larson and Von Dreele, 1994) using the graphical interface EXPGUI (Toby, 2001); the starting atomic coordinates were taken from Au et al. (2007) for the synthetic $Ca_2Sb_2O_7$ compound. Peak profiles were described by a pseudo-Voigt function; the intensity cut-off for the calculation of the profile-step intensity was 1% of the peak maximum. The background was modelled using the Chebyshev polynomial function with 12 parameters. The 2θ zero-shift, sample-shift and peak-asymmetry were refined for the set of data

collected at room temperature (Figure 1) and kept constant for the successive refinements. Least-square cycles were carried out adding gradually the following variables: scale factor, background parameters, unit-cell parameters, peak-shape, and atomic parameters. To reduce the number of refined variables, displacement parameters were refined for groups of sites as A1 and A2, B1 and B2, and O1, O2, and O3. The refinement of the atomic coordinates was carried out up to 1173 K; the refinement of the data collected at 1273 K was instable and the atomic parameters were fixed to the values obtained at 1173 K. The Rietveld refinements yielded good agreement between the experimental and calculated data (Table 1). In Table 2 are reported the unit-cell parameters and in Table 3 the atomic coordinates (together with the isotropic displacement parameters) obtained at different temperatures. CIFs are available from the Authors upon request.

Results and discussion

Unit-cell parameters

The relative expansion of the unit-cell parameters and volume are shown in Figure 2. It appears evident that no phase transition occurs in the temperature range investigated and that only a general thermal expansion affects the lattice parameters.

The data reported in Table 2 fit the following linear equations:

$$a\ (\text{Å}) = 7.2818(7) + 7.07(9) \times 10^{-5}[T]$$
$$(R^2 = 0.998)$$
$$b\ (\text{Å}) = 10.1912(9) + 10.6(1) \times 10^{-5}[T]$$
$$(R^2 = 0.999)$$

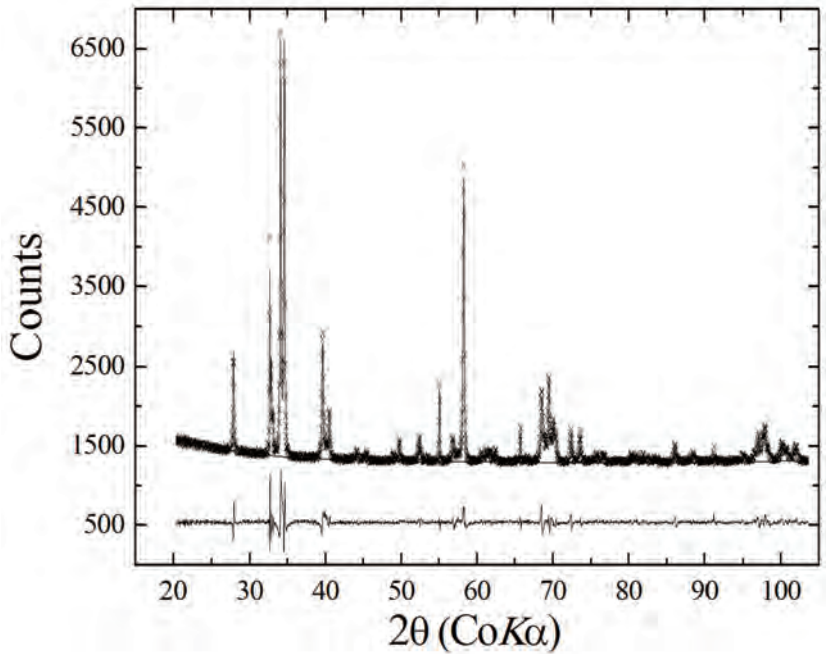

Figure 1. Observed (crosses), calculated (continuous line) and residual (continuous line at bottom) XRD pattern of $Ca_2Sb_2O_7$ at room temperature.

Table 1. Details of the structure Rietveld refinements.

T(K)	298	323	373	473	573	673	773	873	1073	1173	1273*
Rwp (%)	9.69	9.70	9.90	11.83	9.84	10.07	9.88	10.05	10.06	9.84	10.41
Rp (%)	7.34	7.47	7.41	8.91	7.47	7.57	7.38	7.43	7.47	7.27	7.83
$\chi 2$	2.68	2.78	2.96	4.27	2.97	3.16	3.15	3.37	3.47	3.28	3.68
R (F2)	3.05	2.84	2.88	3.23	2.51	2.92	2.92	2.88	2.99	2.89	3.42

Note: *atomic parameters were fixed to the values obtained at 1173 K.

$$c\ (\text{Å}) = 7.4430(6) + 5.80(7) \times 10^{-5}[T]$$
$$(R^2 = 0.998)$$
$$V\ (\text{Å}^3) = 552.4(1) + 0.0155(2)\ [T]$$
$$(R^2 = 0.998)$$

The mean coefficients of thermal expansion along the various axes $\alpha_a = 9.49 \times 10^{-6}\ K^{-1}$, $\alpha_b = 10.11 \times 10^{-6}\ K^{-1}$, $\alpha_c = 7.56 \times 10^{-6}\ K^{-1}$ and the bulk thermal expansion coefficient $\alpha_V = 27.20 \times 10^{-6}\ K^{-1}$.

Crystal structure

In the structure of the orthorhombic $Ca_2Sb_2O_7$ the pairs of *M* and *N* layers are stacked along [012] (Figure 3). There are two independent large cavities (A1 and A2) hosting Ca and two octahedral sites (B1 and B2) which accommodate Sb^{5+}. Selected bond distances at different temperatures are given in Table 4. Only slight changes occur in the individual bond distances without evidence of abrupt structural changes, with a general trend to increase of <A2-O> and <B2-O>, in particular. The two shortest distances (A1-O2), which connect adjacent layers, remain basically unchanged from room temperature [2.23(3) Å] to 1173 K [2.21(3) Å]. As a result, because the A1-O2 distances are directed along

Table 2. Unit-cell parameters of the synthetic $Ca_2Sb_2O_7$ from 298 to 1273K.

T (K)	*a* (Å)	*b* (Å)	*c* (Å)	*V* (Å3)
298	7.3043(2)	10.2253(4)	7.4611(2)	557.26(2)
323	7.3055(2)	10.2273(4)	7.4620(2)	557.53(2)
373	7.3072(2)	10.2299(3)	7.4636(2)	557.92(2)
473	7.3157(2)	10.2408(4)	7.4716(2)	559.76(2)
573	7.3214(2)	10.2515(3)	7.4755(3)	561.08(2)
673	7.3280(2)	10.2616(4)	7.4812(2)	562.56(2)
773	7.3354(2)	10.2716(3)	7.4875(2)	564.16(2)
873	7.3431(2)	10.2829(3)	7.4938(2)	565.84(2)
1073	7.3579(2)	10.3055(3)	7.5059(2)	569.15(2)
1173	7.3653(2)	10.3161(3)	7.5115(2)	570.73(4)
1273	7.3722(2)	10.3266(4)	7.5163(2)	572.21(5)

Table 3. Atomic coordinates and isotropic displacement parameters for synthetic $Ca_2Sb_2O_7$ at different temperatures.

T (K)	O1*z*	O2*y*	O2*z*	O3*x*	O3*y*	O3*z*	A*Uiso*	B*Uiso*	O*Uiso*
298	0.181(4)	0.398(2)	0.737(4)	0.207(2)	0.379(2)	0.427(2)	0.020(2)	0.0155(8)	0.020(4)
323	0.179(4)	0.401(2)	0.731(4)	0.206(2)	0.382(2)	0.430(2)	0.021(2)	0.0155(8)	0.027(4)
373	0.181(4)	0.400(2)	0.734(4)	0.208(2)	0.381(2)	0.428(2)	0.019(1)	0.0157(8)	0.017(4)
473	0.179(4)	0.401(2)	0.735(4)	0.205(2)	0.383(2)	0.428(2)	0.013(2)	0.012(1)	0.007(4)
573	0.178(4)	0.398(2)	0.738(3)	0.206(2)	0.381(1)	0.427(2)	0.023(2)	0.0172(8)	0.019(4)
673	0.177(4)	0.400(2)	0.736(3)	0.207(2)	0.382(2)	0.427(2)	0.029(2)	0.0204(8)	0.019(4)
773	0.180(4)	0.400(2)	0.740(3)	0.208(2)	0.382(1)	0.424(2)	0.028(2)	0.0201(8)	0.020(4)
873	0.174(4)	0.399(2)	0.740(4)	0.208(2)	0.381(1)	0.425(2)	0.029(2)	0.0221(8)	0.023(4)
1073	0.177(4)	0.396(2)	0.742(4)	0.208(2)	0.379(1)	0.420(2)	0.035(2)	0.0219(8)	0.026(4)
1173	0.171(4)	0.395(2)	0.743(4)	0.207(2)	0.378(1)	0.419(2)	0.038(2)	0.0215(8)	0.028(4)

Notes: space group *Imma*, A1 on (0,0,0), A2 on (1/4,1/4,3/4), B1 on (1/4,1/4,1/4), B2 on (0,0,1/2), O1 on (0,1/4,z), O2 on (0,y,z) and O3 on (x,y,z).

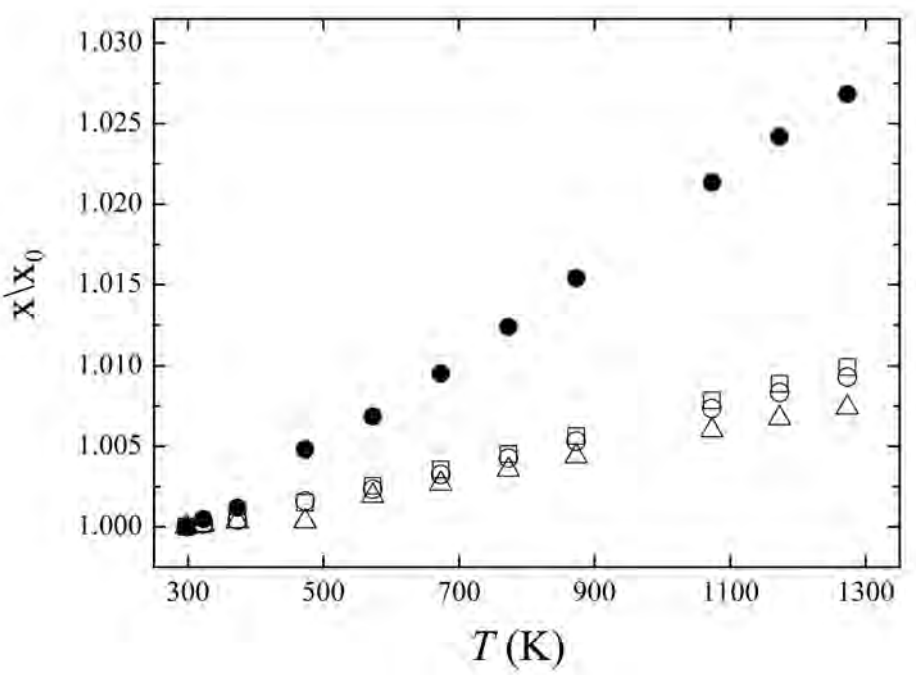

Figure 2. Relative expansion of the unit-cell parameters (empty symbols) and volume (full circles) in the temperature range 298-1273 K. Note that *a* (circles) and *b* (squares) parameters show a slightly greater increase with respect to the *c* parameter (triangles). Errors within the symbol size.

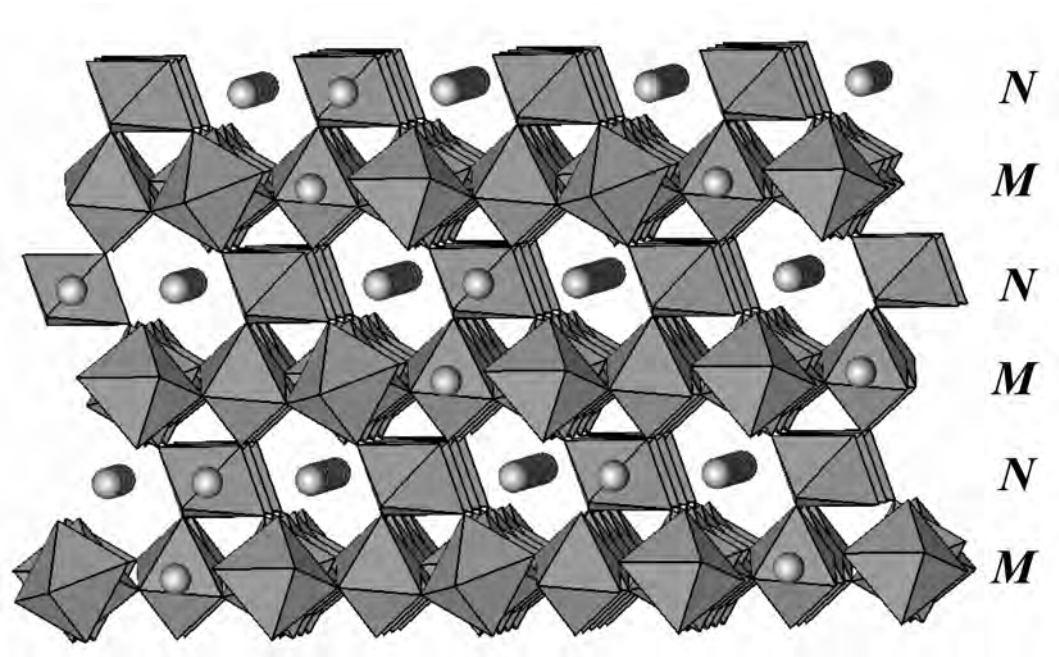

Figure 3. Stacking along [012] of *M* and *N* layers in the structure of orthorhombic $Ca_2Sb_2O_7$. View approximately along [11$\bar{1}$].

Table 4. Selected bond distances (Å) for synthetic $Ca_2Sb_2O_7$ from 298 to 1173 K.

T(K)	298	323	373	473	573	673	773	873	1073	1173
A1-O1(x2)	2.89(1)	2.89(1)	2.89(1)	2.89(1)	2.89(1)	2.89(1)	2.90(1)	2.88(1)	2.90(1)	2.88(1)
O2(x2)	2.23(3)	2.25(3)	2.24(3)	2.22(3)	2.22(3)	2.23(3)	2.21(3)	2.21(3)	2.22(3)	2.21(3)
O3(x4)	2.53(2)	2.52(2)	2.52(2)	2.50(2)	2.54(1)	2.53(2)	2.53(2)	2.54(2)	2.56(2)	2.57(2)
<A1-O>	2.55	2.55	2.55	2.53	2.55	2.55	2.55	2.54	2.56	2.55
A2-O2(x4)	2.37(1)	2.40(1)	2.39(1)	2.40(1)	2.38(1)	2.39(1)	2.39(1)	2.39(1)	2.38(1)	2.37(1)
O3(x4)	2.77(1)	2.76(1)	2.77(1)	2.78(2)	2.78(1)	2.79(1)	2.81(1)	2.80(1)	2.83(1)	2.83(1)
<A2-O>	2.57	2.58	2.58	2.59	2.58	2.59	2.60	2.60	2.61	2.60
B1-O1(x2)	1.897(7)	1.901(8)	1.887(8)	1.903(8)	1.908(7)	1.911(8)	1.907(7)	1.921(8)	1.920(8)	1.935(9)
O3(x4)	1.89(2)	1.93(2)	1.91(2)	1.90(2)	1.91(2)	1.92(2)	1.90(1)	1.91(2)	1.87(2)	1.86(2)
<B1-O>	1.89	1.92	1.90	1.90	1.91	1.92	1.90	1.91	1.89	1.89
B2-O2(x2)	2.06(3)	2.00(2)	2.02(2)	2.03(3)	2.05(2)	2.05(2)	2.07(2)	2.08(3)	2.11(3)	2.12(3)
O3(x4)	2.03(1)	2.00(1)	2.02(1)	2.02(2)	2.02(1)	2.01(1)	2.03(1)	2.03(2)	2.06(1)	2.07(1)
<B2-O>	2.04	2.00	2.02	2.02	2.03	2.02	2.04	2.05	2.08	2.09

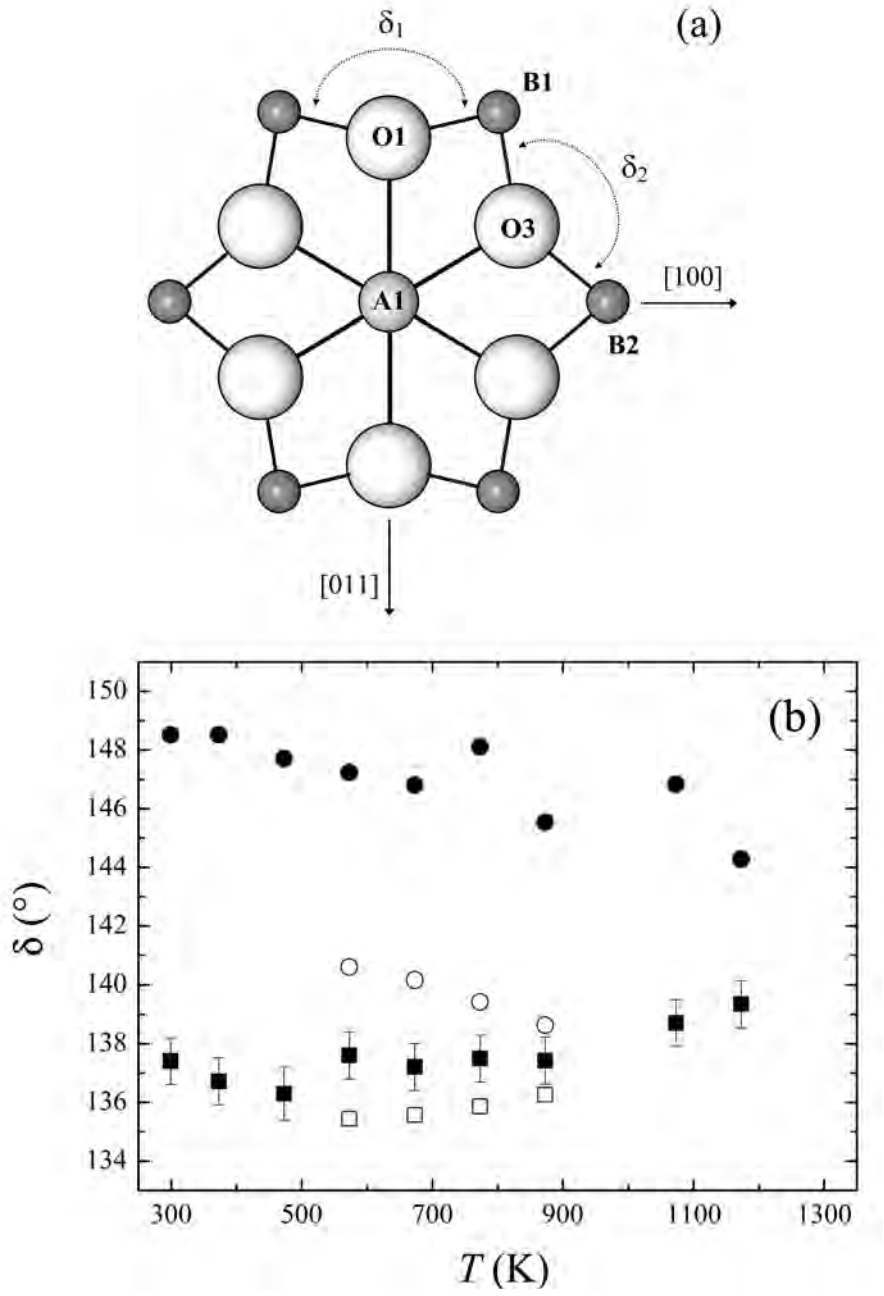

Figure 4. a) Pseudo-hexagonal arrangement of the alternating B cations and anions surrounding the A1 cation in the *M* layer (A1 on 2/*m* symmetry site); b) variation of δ_1 (circles) and δ_2 (squares) angles with the increase of temperature: full symbols refer to $Ca_2Sb_2O_7$ (this study) and empty symbols refer to $Ca_2Os_2O_7$ (Reading et al., 2002).

[013] and [0$\bar{1}$3] in the *M* and *N* layers respectively, the expansion along the c-axis is less pronounced. Being O2 the most underbonded oxygen atom of the structure, the A1-O2 bonds act as a constraint to the expansion in their direction. This structural feature is consistent with the variations of the unit-cell parameters described above. The increase of temperature induces variations in the pyrochlore-like *M* layer. In Figure 4a the pseudohexagonal arrangement of alternating octahedral cations (B1 and B2) and anions (O1 and O3) surrounding the A1 cation is shown; with the increase of temperature, the δ_1 and δ_2 independent angles converge towards similar values (Figure 4b). An analogous trend toward a regularization was observed in the structure of synthetic $Ca_2Os_2O_7$ (Reading et al., 2002).

Acknowledgements

The paper has benefited by the official reviews made by Alessandro Gualtieri and one anonymous reviewer. This research was supported by M.I.U.R., cofinanziamento 2007, project "Complexity in minerals: modulation, phase transition, structural disorder" issued to Silvio Menchetti, and by C.N.R., Istituto di Geoscienze e Georisorse, sezione di Firenze, Italy.

References

Au Y.S., Fu W.T. and Ijido D.J.W. (2007) - Crystal structure of $Ca_2Ln_3Sb_3O_{14}$ (Ln = La, Pr, Nd and Y); A novel variant of weberite. *Journal of Solid State Chemistry*, 180, 3166-3171.

Bonazzi P. and Bindi L. (2007) - The crystal structure of ingersonite, $Ca_3Mn^{2+}Sb^{5+}{}_4O_{14}$, and its relationships with pyrochlore. *American Mineralogist*, 92, 947-953.

Brisse F., Stewart D.J., Seidl V. and Knop O. (1972) - Pyrochlores. VIII. Pyrochlores and related compounds and minerals. *Canadian Journal of Chemistry*, 50, 3648-3666.

Cai L. and Nino J.C. (2009) - Complex Ceramic Structures. I. Weberites. *Acta Crystallographica*, B65, 269-290.

Coelho A.A., Cheary R.W. and Smith K.L. (1997) - Analysis and structural determination of Nd-substituted zirconolite-4M. *Journal of Solid State Chemistry*, 129, 346-359.

Gatehouse B.M., Grey I.E., Hill R.J. and Rossell H.J. (1981) - Zirconolite, $CaZr_xTi_{3-x}O_7$; structure refinements for near-end-member compositions with x = 0.85 and 1.30. *Acta Crystallographica*, B37, 306-312.

Giuseppetti G. and Tadini C. (1978) - Re-examination of the crystal structure of weberite. *Tschermaks Mineralogische und Petrographische Mitteilungen*, 25, 57-62.

Grey I.E. and Roth R.S. (2000) - New calcium tantalate polytypes in the system $Ca_2Ta_2O_7$-$Sm_2Ti_2O_7$. *Journal of Solid State Chemistry*, 150, 167-177.

Grey I.E., Mumme W.G., Ness T.J., Roth R.S. and Smith K.L. (2003) - Structural relations between weberite and zirconolite polytypes - refinements of doped 3T and 4M $Ca_2Ta_2O_7$ and 3T $CaZrTi_2O_7$. *Journal of Solid State Chemistry*, 174, 285-295.

Ismunandar I. and Budiman Y. (2002) - Temperature dependent X-ray powder diffraction study of $Pb_{2.5}Sb_{1.5}O_{6.75}$. *Indonesian Journal of Physics*, 13, 162-164.

Knop O., Demazeau G. and Hagenmuller P. (1980) - Pyrochlores. XI. High-pressure studies of the antimonates $A_2Sb_2O_7$ (A = Ca, Sr, Cd) and preparation of the weberite $Sr_2Bi_2O_7$. *Canadian Journal of Chemistry*, 58, 2221-2224.

Larson A.C. and Von Dreele R.B. (1994) - GSAS Generalized Structure Analysis System. LAUR86-748, Los Alamos National Laboratory, Los Alamos, NM-87545.

Mazzi F. and Munno R. (1983) - Calciobetafite (new mineral of the pyrochlore group) and related minerals from Campi Flegrei, Italy; crystal structures of polymignyte and zirkelite: comparison with pyrochlore and zirconolite. *American Mineralogist*, 68, 262-276.

Reading J., Knee C.S. and Weller M.T. (2002) - Syntheses, structures and properties of some osmates (IV, V) adopting the pyrochlore and weberite structures. *Journal of Materials Chemistry*, 12, 2376-2382.

Scott H.G. (1990) - Refinement of the crystal structure of the manganese antimonate $Mn_2Sb_2O_7$ with neutron powder diffraction data by the profile decomposition

method. *Zeitschrift für Kristallographie*, 190, 41-46.

Smith K.L. and Lumpkin G.R. (1993) - Structural features of zirconolite, hollandite and perovskite, the major waste-bearing phases in Synroc. In: Defects and Processes in the Solid State: Geoscience Applications. The McLaren Volume, Bolan J.N. and FitzGerald J.D. (eds), Elsevier, Amsterdam, 401-422.

Swenson C.A. (1983) - Recommended values for the thermal expansivity of silicon from 0 to 1000 K. *Journal of Physical and Chemical Reference Data*, 12, 179-182.

Toby B.H. (2001) - EXPGUI, a graphical user interface for GSAS. *Journal of Applied Crystallography*, 34, 210-213.

Yakubovich O.V., Urusov V.S., Massa W., Frenzen G. and Babel D. (1994) - Crystal-chemical relations in weberite-group minerals, $Na_2M^{II}M^{III}F_7$, as derivatives of fluorite. *Geologiya*, 6, 19-25 (in Russian, English abstract).

Submitted, October 2010 - Accepted, January 2011